Impacts of Coastal SST Variability on the East Asian Summer Monsoon

HUANG Anning (黄安宁), ZHANG Yaocun* (张耀存), and GAO Xinfang (高新房)

Department of Atmospheric Sciences, Nanjing University, Nanjing 210093

ABSTRACT

The impacts of the seasonal and interannual SST variability in the East Asia coastal regions (EACRSST) on the East Asian summer monsoon (EASM) have been examined using a regional climate model (PσRCM9) in this paper. The simulation results show that the correlation between the EACRSST and the EASM is strengthened after the mid-1970s and also the variability of the EACRSST forcing becomes much more important to the EASM interannual variability after the mid-1970s. The impacts of the EACRSST on the summer precipitation over each sub-region in the EASM region become weak gradually from south to north, and the temporal evolution features of the summer precipitation differences over North and Northeast China agree well with those of the index of EASM (IEASM) differences.

The mechanism analyses show that different EACRSST forcings result in the differences of sensible and latent heat flux exchanges at the air-sea interface, which alter the heating rate of the atmosphere. The heating rate differences induce low level air temperature differences over East Asia, resulting in the differences of the land-sea thermal contrast (LSTC) which lead to 850 hPa geopotential height changes. When the 850 hPa geopotential height increases over the East Asian continent and decreases over the coast of East China and the adjacent oceans during the weakening period of weakens consequently. On the contrary, the EASM enhances during the strengthening period of the LSTC.

Key words: SST variability, coastal oceans, East Asian monsoon, numerical simulations

DOI: 10.1007/s00376-007-0259-7

1. Introduction

The East Asian summer monsoon (EASM) is an important large-scale circulation pattern arising from the thermal contrast between the warmer Asian continent and the adjacent cooler ocean. The year-to-year variation of the EASM has a close relationship with the floods and droughts over East China in summer (Zhu, 1934; Ding, 1994; Guo, 1994), which induces large economic losses. For example, the rainfall increases dramatically over the Yangtze and Huaihe River valley and decreases over North China in the weak EASM years, but the case is reversed in the strong EASM years (Shi et al., 1996; Zhu and Wang, 2001; Guo et al., 2003; Lu et al., 2004). Therefore, substantial efforts have been devoted during the past several decades into investigating the variation of the EASM and the related mechanisms from various viewpoints. Besides considering the dynamical processes operating within the atmosphere itself, more investi-

gations have been made to regard the variability of the EASM as the major results of the external forcing, such as ENSO, the thermal condition anomalies of the western Pacific warm pool, dynamic and thermal characteristic variations of the Tibetan Plateau, and the increase/decrease in Eurasian continent snow cover (Huang and Huang, 1999; Huang et al., 2003; Qian et al., 2003). It is well known that the land-sea thermal contrast (LSTC) is the fundamental reason for the monsoon circulation formation. The East Asian continent is surrounded by the western Pacific, the South China Sea and the Indian Ocean, from east to south. As a consequence, there exists a zonal LSTC between the Asian continent and the western Pacific, and a meridional LSTC between the Asian continent and the Indian Ocean, and the basinwide South China Sea (SCS). With the warmest SST among the global oceans and strong air-sea interaction processes, the thermal features of the western Pacific warm pool exert a significant impact on the interannual variabil-

ity of the EASM (Nitta, 1987; Kurihara, 1989; Huang and Sun, 1992, 1994; Jin and Chen, 2002; Huang et al., 2005). The studies of Xue (2001) showed that the air-sea interaction over the western Pacific and Indian Ocean plays an important role in the interannual to interdecadal variation of the EASM. Li and He (2001, 2002) pointed out that the meridional circulation over East Asia is closely coupled with the low-latitude zonal circulation after 1976, which strengthens the correlation between the EASM and SST anomaly (SSTA) in the middle-eastern Pacific. The SSTA over the middle-eastern Pacific during the previous winter affects the EACRSSTA in the next summer, and subsequently influences the rainfall over the mid-lower reaches of the Yangtze River valley. Along with the observational analyses, many numerical investigations have also proved that the SST anomalies in geographically localized regions such as the western Pacific and Indian Ocean have a strong influence on the EASM (Zhang and Qian, 2002; Liang and Wu, 2003; Sun and Ma, 2003).

Recent research suggests that the dynamic and thermal features along the coastal oceans of Asia also have a notable relationship with the seasonal to interannual variations of the EASM (Wang and Qian, 1995; Ren and Qian, 1999; Sun and Ding, 2003). However, the mechanism of the coastal water's impact on the EASM variation is still poorly understood. Thus, the impacts of the seasonal and interannual SST variability in the East Asian coastal regions (EACRSST) on the EASM based on the different climatological backgrounds of the East Asian monsoon are investigated by a regional climate model in this paper. The associated mechanisms are also addressed.

The paper is organized as follows: the P-σ regional climate model (PσRCM9) used in this study and the numerical experiment schemes are described briefly in section 2. The simulation results are presented in section 3. The possible mechanism analyses are provided in section 4. Finally, the concluding remarks are given in section 5.

2. Model description and numerical experiment schemes

The PσRCM9 used in this study is based on a primitive equation model with a P-σ vertical coordinate system. It was first developed by Kuo and Qian (1981, 1982) for investigating the diurnal changes of weather and climate in the development of monsoon circulation over East Asia, and thereafter improved by Qian (1985), Zhang and Qian (1999), Liu and Qian (1999); Liu et al. (2002) and Wang and Qian (2002). The PσRCM9 has 9 vertical atmospheric layers with

a horizontal resolution of $1° \times 1°$. The pressure coordinate is used above 400 hPa with four uniform layers. Below 400 hPa, the σ and σ_b coordinates are adopted. Four σ layers are uniformly divided with $\Delta\sigma = 0.25$, and only one layer is defined as the atmospheric boundary layer with a 50 hPa thickness in the σ_b coordinate. The model domain is from $0°$ to $60°$N in latitude and from $70°$E to $140°$E in longitude, including the Tibetan Plateau, the Bay of Bengal, the South China Sea and part of the western Pacific. The model includes a planetary boundary-layer parameterization process, Kuo-type cumulus parameterization scheme (Anthes, 1977) and a detailed atmospheric radiation process. The PσRCM9 and the previous versions have been extensively and successfully used to simulate the large-scale circulations and to investigate the impacts of the air-sea feedback on the atmospheric circulations (Wang and Qian, 2002; Zhang and Perrie, 2001; Ren and Qian, 2005).

In this paper, three simulations have been performed from January 1958 to December 1997, with the same initial and lateral boundary conditions. The initial conditions and boundary conditions, including wind, air temperature, specific humidity, geopotential height fields, are specified by the National Centers for Environmental Prediction/National Center for Atmospheric Research (NCEP/NCAR) reanalysis (Kalnay et al., 1996) monthly mean data. The control run (denoted CTRL) is carried out by using the monthly NCEP/NCAR reanalysis SST from January 1958 to December 1997, as the oceanic boundary forcing. The SST is interpolated into the PσRCM9 grids by using a bilinear interpolation method. Therefore, the seasonal and interannual variability of the EACRSST forcing are included in CTRL. Sensitivity experiments denoted as SENEXP1 and SENEXP2 hold the same initial and lateral boundary conditions as CTRL. However, the climatological monthly mean SST is taken as the oceanic boundary forcing in SENEXP1, which presents only the seasonal cycle of EACRSST forcing, compared with CTRL. The 480-month mean SST is time-invariant during the whole integration period, taken as the oceanic boundary forcing in SENEXP2. Consequently, the seasonal and interannual variability is entirely removed in SENEXP2. For all the experiments, the nudging technique is applied only in the lateral boundary outer ten grids.

3. The simulation results

3.1 *Overview of the simulated EASM and precipitation*
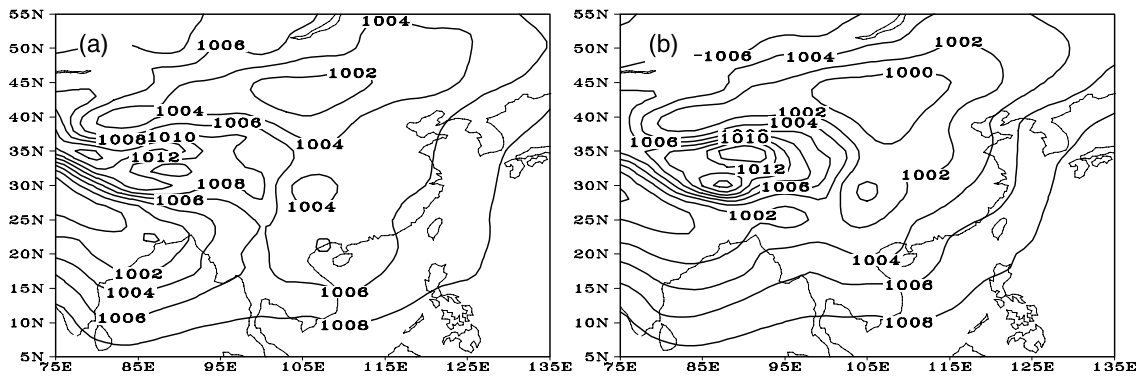
Numerical simulations (Wang, 2001b; Huang and

Fig. 1. Distributions of the sea level pressure in summer averaged over 1958–1997: (a) NCEP/NCAR reanalysis data; (b) CTRL (Units: hPa)
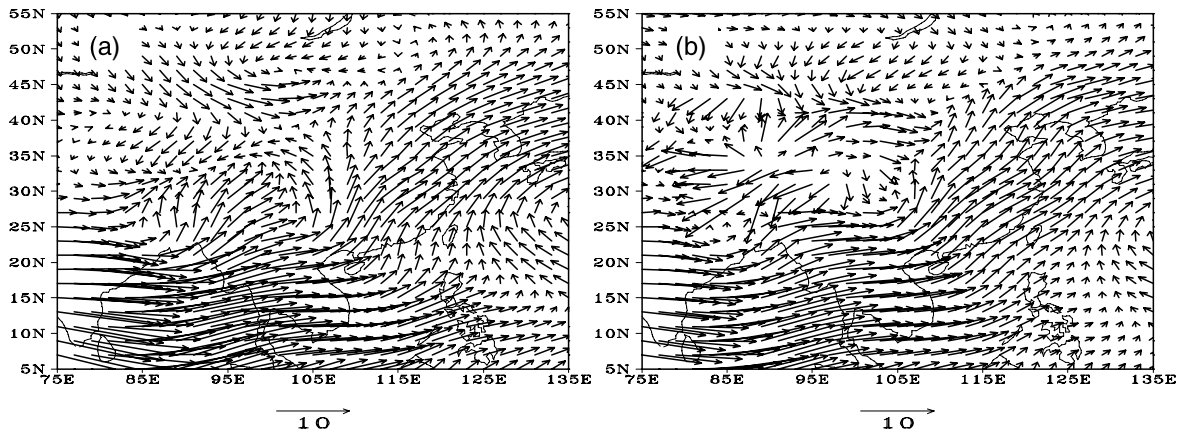

Fig. 2. As in Fig. 1, except for 850 hPa wind (Units: m s^{-1}).

Zhang, 2004) have shown that the PσRCM9 has good performance in simulating climatological characteristics over East Asia and the associated seasonal to interannual variability of geopotential height and air temperature. However, the model's performance in representing the EASM and its variation has not been examined systematically. Therefore, it is necessary to validate the PσRCM9 performance in simulating the EASM and the variation first. In this section, the simulated monsoon circulation and the accompanying precipitation are respectively compared with the NCEP/NCAR reanalysis data and the observed monthly mean precipitation from the World Meteorological Organization surface networks with 160 stations in China.

Figures 1b and 2b show respectively the simulated sea level pressure and low-level wind vectors in CTRL during the summer season (June–July–August) averaged from 1958 to 1997. The corresponding observational results are depicted in Figs. 1a and 2a, respectively. Generally speaking, the PσRCM9 repro-

duces the distribution pattern of the sea level pressure over Asia and the adjacent regions well, except that the sea level pressure over mid-latitude East China is slightly underestimated by about 2 hPa. Figure 2a illustrates the low-level southwest wind extending northeastwards from the Bay of Bengal to 50°N, which is one of the typical features of the EASM. It is seen from Fig. 2b that the CTRL simulations indicate similar characteristics as the observations, especially the monsoon flow over the low latitudes and East Asia.

The observation-to-model comparison of the summer precipitation averaged from 1958 to 1997 is shown in Figs. 3a and 3b, respectively. As indicated above, the distribution of the summer precipitation over East China is strongly related with the EASM circulation. Figure 3a shows that the observed summer precipitation over East China is reduced from south to north dramatically and the maximal precipitation center is located in South China. The CTRL simulation in Fig. 3b also presents the northward decreasing distribution of the monsoon precipitation in China. However, the
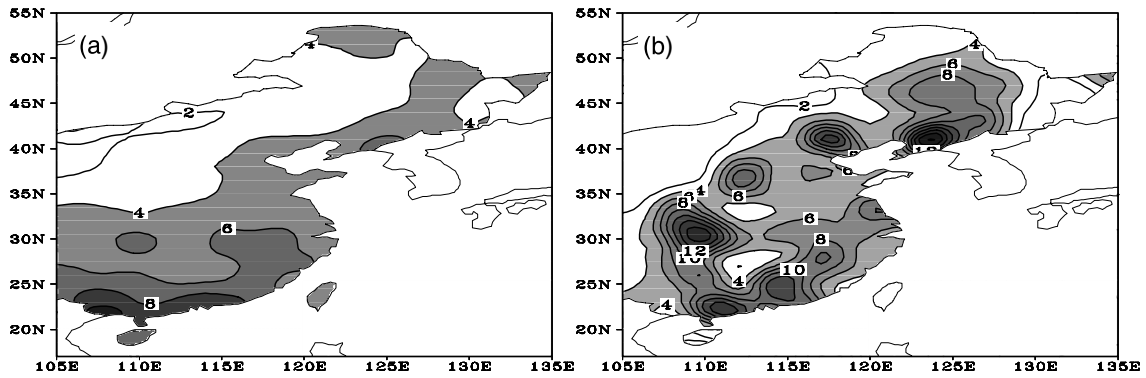
Fig. 3. Distributions of the summer precipitation over East China averaged over 1958–1997: (a) observationl; (b) CTRL (Units: mm d^{-1}).
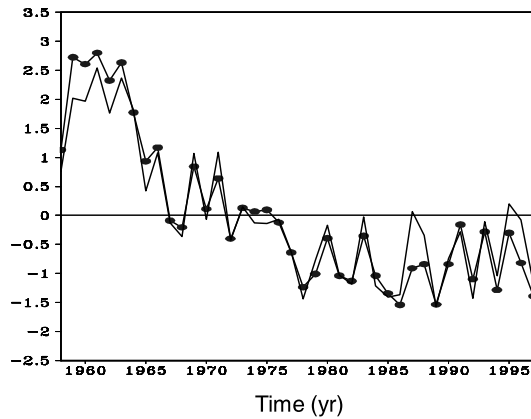

Fig. 4. Temporal variation of the IEASM in CTRL and NCEP/NCAR reanalysis, with solid line for NCEP/NCAR reanalysis and solid line with solid circles for CTRL (Units: m s^{-1}).

model-simulated precipitation is relatively larger than the observations, especially in North China.

It is well known that the EASM is an extremely complex phenomenon, which is comprised of tropical and subtropical components (Zhu, 1986). The present study focuses on the impacts of the EACRSST on the subtropical circulations of the EASM. A concise and effective index denoted "IEASM" for describing the regionally-averaged southwest wind feature is defined by Wang (2000):

$$\text{IEASM} = \overline{(u' + v')/\sqrt{2}}, \qquad (1)$$

where u' and v' are the summer zonal and meridional wind departures from the climatological mean, averaged over a certain area. The key domain of EASM，as in Wang (2000) and Xue (2001)，is confined to 20°–40°N, 110°–125°E. It is obvious that the IEASM describes the regionally-averaged southwest wind anomaly with a clear physical meaning and a simple method of calculation.

Based on the NCEP/NCAR reanalysis and CTRL simulation, the above index has a record length of 40 yr, thus permitting a reasonable statistical estimate of the EASM variability and observation-to-model comparison. Figure 4 suggests that the simulated IEASM agrees well with the observations. The correlation coefficient of the observations with CTRL is 0.96, highly significant at the 99% confidence level. The IEASM tends to decline from a strong stage in the mid-1960s to a weak stage after the mid-1970s. This is consistent with the recent findings of Xue (2001) and Wang (2001a).

As the lateral boundary in a regional climate simulation is expected to affect the simulated monsoon circulation, an additional test run, in which the model domain is stretched outwards with ten grids and the nesting technique is still applied only to the outer ten grids, is conducted in order to ascertain whether the lateral boundary effects on the IEASM simulation are negligible. The results show that the PσRCM9 still reproduces the IEASM properly (not shown)，indicating that the lateral boundary is not a serious problem for the IEASM simulation.

In summary, it is evident that the PσRCM9 portrays a reasonable EASM circulation over Asia and adjacent oceans, as well as the associated precipitation distribution over China. The PσRCM9 also depicts the temporal variation of the EASM during the period from 1958 to 1997, suggesting that it provides an effective tool for investigating the impacts of the EACRSST on the EASM.

3.2 IEASM differences between CTRL and SENEXP1, SENEXP2

It is noted that the IEASM differences between CTRL and SENEXP1 represent the impacts of the interannual EACRSST variability on the EASM, and the IEASM differences between SENEXP1 and SENEXP2 reflect the influences of the seasonal EACRSST
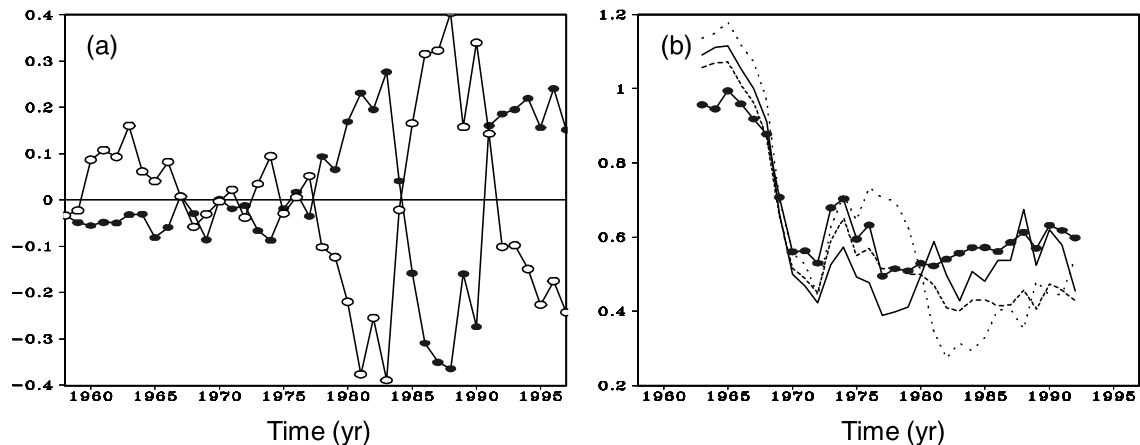
Fig. 5. (a) Temporal evolution of the IEASM differences simulated under different EACRSST forcings (solid line with solid circles for the differences between CTRL and SENEXP1 and solid line with open circles for the differences between SENEXP1 and SENEXP2); (b) the 11-year moving standard deviations of the IEASM in the three experiments and NCEP/NCAR reanalysis (solid line with solid circles for NCEP/NCAR reanalysis, solid line for CTRL, dotted line for SENEXP1 and dashed line for SENEXP2) (Units: m s^{-1}).

variability on the EASM. As shown in Fig. 5a, the IEASM difference is weak before the mid-1970s. The maximum difference is no more than 0.2 m s^{-1}, suggesting a tenuous relationship between the EACRSST and the EASM during this period. The IEASM differences experience a sudden increase after the mid-1970s compared to before, indicating the strengthening of the linkage between the EACRSST and the EASM after the mid-1970s, which is consistent with the results obtained by Li and He (2001, 2002). The correlation coefficient of the two curves in Fig. 5a is -0.897, suggesting that the seasonal and interannual variability of the EACRSST have opposite impacts on the EASM.

In order to identify the effects of the SST apart from the variability of the wind fields provided by lateral boundaries, two additional test runs with climatological lateral boundary conditions forced by observed and climatological SST, respectively, were performed. The results show that the IEASM differences of these two experiments are very consistent with those of CTRL and SENEXP1 (not shown). This indicates that the IEASM differences are mainly caused by SST forcing and are negligibly affected by the variability of the wind fields.

Figure 5b shows the 11-year moving standard deviations of the IEASM in the three experiments, which depict the long-term variability by smoothing the high-frequency noise. Overall, the moving standard deviations of the IEASM in the three experiments indicate considerable variations. On the other hand, the EASM tends to decline from a stage with larger interannual variability in the mid-1960s to a stage with weak interannual variability after the mid-1970s, both of

which are in good agreement with the NCEP/NCAR reanalysis. Under different EACRSST forcing, the EASM interannual variability differences strengthen after the mid-1970s, indicating that the variability of the EACRSST forcing became much more important to the EASM interannual variability after the mid-1970s.

3.3 The summer precipitation differences over East China

As mentioned earlier, the EASM consists of many regional subcomponents, leading to a distinctive precipitation distribution over different regions (Shi et al., 1996; Zhu and Wang, 2001; Guo et al., 2003; Lu et al., 2004). For a detailed examination of the precipitation differences among the three experiments over different regions, we divide East China (20°–27°N, 105°–120°E) into four sub-regions according to the regional monsoon rainfall characteristics: South China (20°–27°N, 105°–120°E), the mid-lower reaches of the Yangtze River valley (27°–35°N, 105°–120°E), North China (35°–42°N, 105°–120°E) and Northeast China (42°–50°N, 105°–120°E).

The simulated summer precipitation differences over each sub-region for different EACRSST forcings are shown in Fig. 6. Similar to the discussion of Fig. 5a, the correlation coefficients of the summer precipitation differences between CTRL and SENEXP1 and between SENEXP1 and SENEXP2 over all sub-regions are negative, suggesting that the EACRSST seasonal variability and interannual variability play opposite roles in the summer precipitation variation over each sub-region. It is also shown that the impacts of the
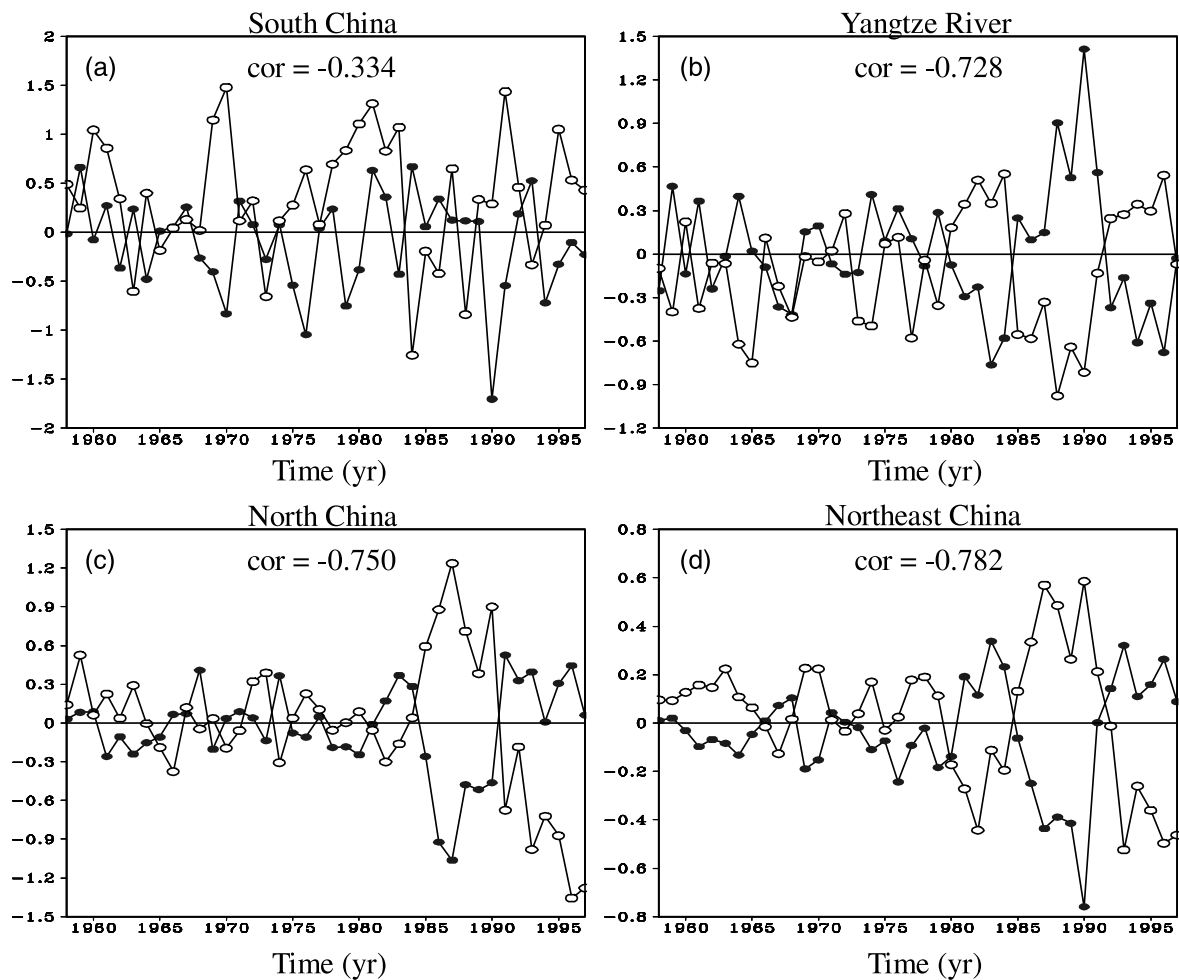
Fig. 6. Temporal variation of the summer precipitation differences over each sub-region of East China in summer simulated under different EACRSST forcings (Units: mm d^{-1}). Solid line with solid circles is the difference between CTRL and SENEXP1 and solid line with open circles is the difference between SENEXP1 and SENEXP2. The sign "cor" denotes correlation coefficient.
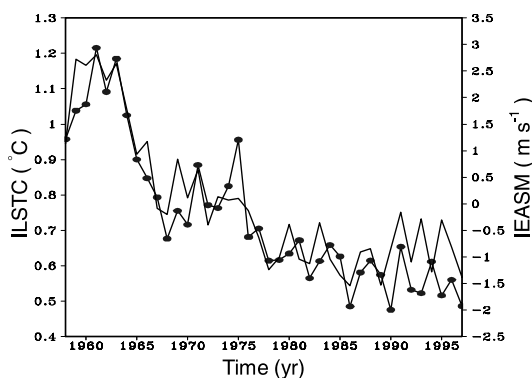

Fig. 7. Temporal variation of the IEASM (solid line in units of m s^{-1} and corresponding to the right axis label) and the ILSTC (solid line with solid circles in units of °C and corresponding to the left axis label) in CTRL experiment.

EACRSST on the summer precipitation over East China become weak gradually from south to north as a whole. Meanwhile, the temporal evolution features of the summer precipitation differences over North China (Fig. 6c) and Northeast China (Fig. 6d) agree with those of the IEASM differences (Fig. 5a) after 1980: the summer precipitation decreases over North and Northeast China during the weakening period of the EASM, but the case is reversed during the strengthening period of the EASM. It is necessary to point out that the summer precipitation differences over the mid-lower reaches of the Yangtze River valley (Fig. 6b) have similar features as those over North and Northeast China because of the deficiency of PσRCM9, which cannot simulate the negative correlation between the EASM and the summer precipitation over the mid-lower reaches of the Yangtze River
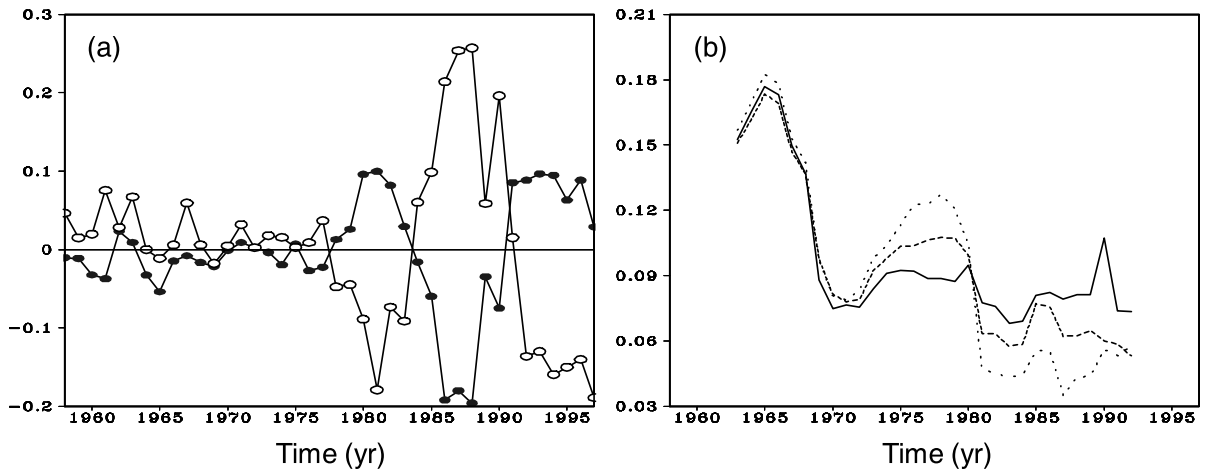
Fig. 8. (a) Time evolution of the ILSTC differences simulated under different EACRSST forcings (solid line with solid circles for the differences between CTRL and SENEXP1 and solid line with open circles for the differences between SENEXP1 and SENEXP2); and (b) the 11-year moving standard deviations of the ILSTC in the three experiments (solid line for CTRL, dotted line for SENEXP1 and dashed line for SENEXP2). (Units: °C)

valley.

4.   Possible mechanism

In section 3, we showed a clear relationship between the seasonal and interannual variability of the EACRSST and the EASM, and also the associated summer precipitation in China. Here, we try to understand the thermodynamic mechanism, particularly, the linkage between the heating rate variation over the East Asian continent and the adjacent oceans, and the EASM.

As mentioned above, the EASM is principally maintained by the temperature contrast between the warmer continent and cooler oceans. It is natural to expect an alteration of the EASM when increasing/decreasing the land-sea thermal contrast (LSTC). An additional idealized experiment with no LSTC through covering the domain with water is conducted to investigate the impacts of the land/sea contrast on the EASM, which is similar to the experiment of Yoshikane and Yoshikane and Kimura (2001). As expected, the simulation result is characterized by no mark of the EASM, attributed to the absence of the LSTC (not shown). Therefore, it is of significance to examine the LSTC differences simulated with different EACRSST forcings.

An index of LSTC (ILSTC), representing the zonal and meridional LSTC, is defined as follows (Sun et al., 2002):

$$\text{ILSTC} = (T_{L1} - T_{O1}) \times \frac{4}{7} + (T_{L2} - T_{O2}) \times \frac{3}{7}, \quad (2)$$

where T_{L1} and T_{L2} are the area-averaged air temper-

ature between 850 hPa and 300 hPa over two land regions (20°–35°N, 105°–120°E; and 20°–27°N, 105°–120°E), respectively, and T_{O1} and T_{O2} are the same as T_{L1} and T_{L2}, but averaged over two ocean regions (15°–30°N, 120°–140°E; and 5°–20°N, 105°–120°E), respectively. Therefore, $(T_{L1} - T_{O1})$ represents the zonal LSTC, and $(T_{L2} - T_{O2})$ evaluates the meridional LSTC quantitatively. The weighting coefficient 4/7 (3/7) for the zonal (meridional) LSTC is taken to emphasize its relative importance.

Figure 7 shows the temporal variation of the IEASM and the ILSTC in the CTRL experiment from 1958 to 1997. The most significant result from the figure is that the interannual variation of the IEASM displays a nearly in-phase variation feature with the ILSTC. The correlation coefficient between them is 0.92, highly significant at the 99% confidence level, indicating that the ILSTC is strongly related with the IEASM. Therefore, the definition of the ILSTC in formula (2) is reasonable.

As shown in Fig. 8a, the ILSTC differences become robust after the mid-1970s, similar to the IEASM differences shown in Fig. 5a. This indicates that the LSTC transition after the mid-1970s plays an extremely influential role in the suddenly-increasing differences of the IEASM shown in Fig. 5a. Meanwhile, the correlation coefficient between the two curves in Fig. 8a is −0.93, implying that the EACRSST seasonal variability and interannual variability play opposite roles in the LSTC variation as well. Figure 8b is the same as Fig. 5b, but for the ILSTC. It is noted that the temporal variation of the ILSTC interannual variability is very similar to that of the IEASM (Fig. 5b), suggesting that the interannual variability of the
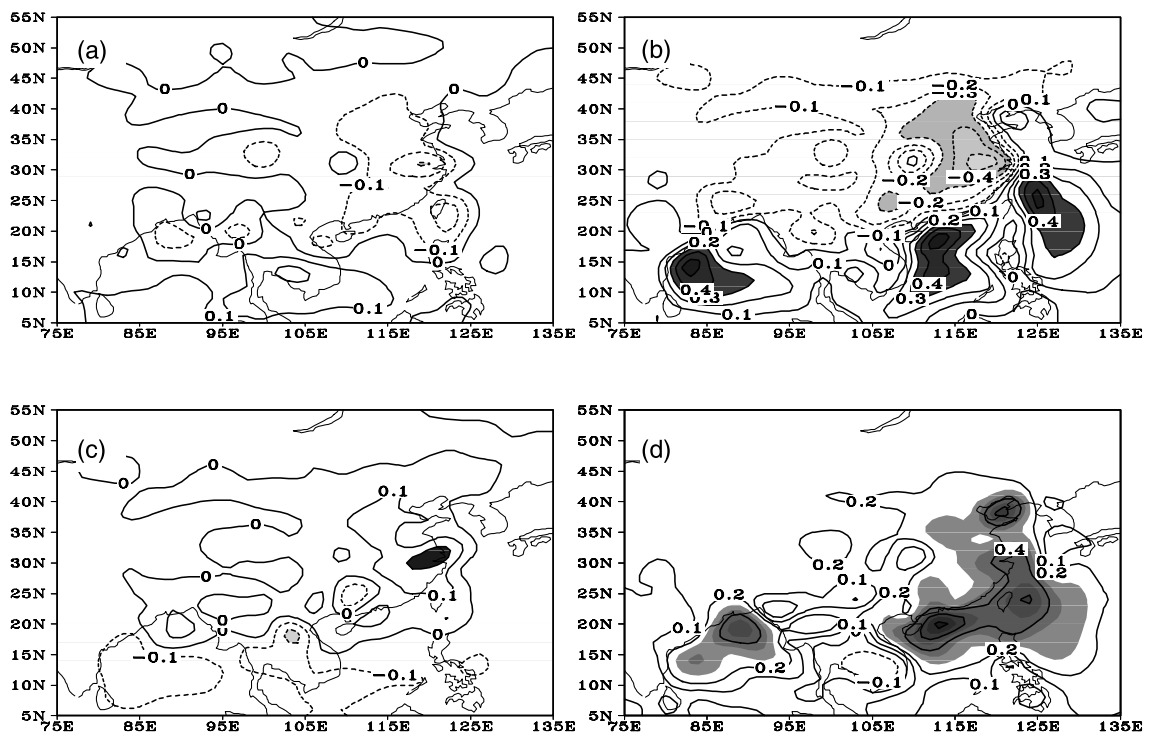
Fig. 9. The differences of the mean heating rate in 850–300 hPa in summer during the (a, b) weakening and (c, d) strengthening periods of the LSTC, regions over the 95% significance level are shaded (Units: $^\circ$C d^{-1}). (a, c) the difference between CTRL and SENEXP1; (b, d) the difference between SENEXP1 and SENEXP2.

LSTC is contributed to by the EASM interannual variability.

The results presented in Figs. 5 and 8 demonstrate that the LSTC has important impacts on the intensity and interannual variability of the EASM. Actually, the EASM variability is strongly associated with the LSTC and they are coincident in nature. To understand the mechanism for the EASM differences, we should discuss what causes the LSTC differences. Firstly, according to Fig. 8a, 13 years (1978–1983 and 1991–1997) and 12 years (1958–1961 and 1984–1990) are selected to construct composite patterns for the strengthening and weakening stages respectively, of the LSTC forced by the interannual variability of the EACRSST. Furthermore, 14 years (1958–1963 and 1984–1991) and 12 years (1978–1983 and 1992–1997) are chosen as the strengthening and weakening periods, respectively, of the LSTC forced by the seasonal variability of the EACRSST.

It is found that the LSTC is closely correlated with the mean heating rate between 850 hPa and 300 hPa (not shown). Different EACRSST forcings result in the differences of the sensible and latent heat flux exchanges at the air-sea interfaces (not shown), which alter the heating rate of the atmosphere. As shown in Figs. 9a and 9b, a negative heating rate difference

center is located over the East Asian continent and a positive one is located over the ocean during the weakening period of the LSTC. This leads to a decrease of the 850 hPa air temperature over the East Asian continent and an increase over the ocean as shown in Figs. 10a and 10b, and consequently this results in the weakening of the temperature contrast in the lower troposphere between the continent and the western Pacific Ocean. However, the heating rate differences have opposite distributions during the strengthening period of the LSTC forced by the interannual variability of the EACRSST (Fig. 9c). The positive heating rate differences are located over both land and ocean as shown in Fig. 9d. This is unlike the distribution shown in Fig. 9c, implying that the land process plays a relatively more important role in the LSTC under the seasonal variability of the EACRSST forcing, compared with the ocean. As shown in Figs. 10c and 10d, the heating rate differences (Figs. 9c and 9d) result in an increase of the 850 hPa air temperature over the East Asian continent and a decrease over the western Pacific Ocean. This intensifies the temperature contrast in the lower troposphere between the continent and the Pacific Ocean. From the analyses of Figs. 8, 9 and 10, it is found that the differences of the mean heating rate between 850 hPa and 300 hPa result in the air
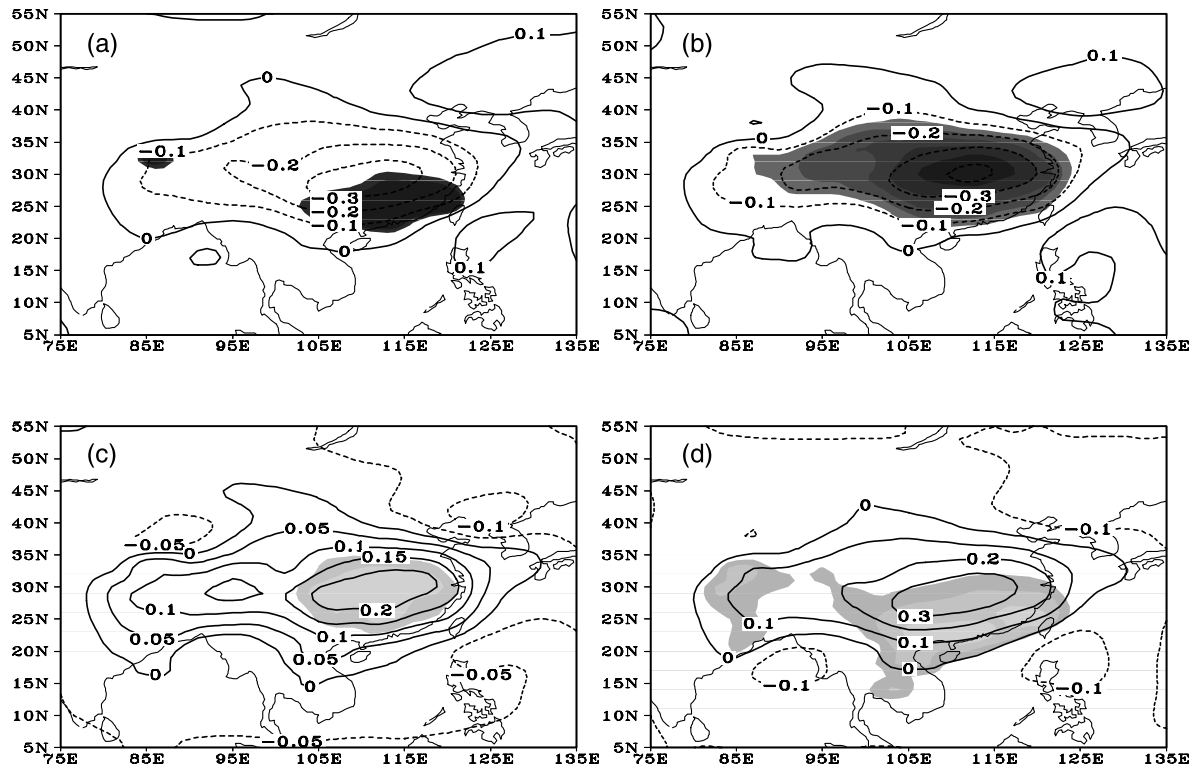
Fig. 10. As in Fig. 9, except for 850 hPa air temperature in summer (Units: °C).

temperature differences in the lower troposphere, and the LSTC changes consequently.

The climatological characteristics of the 850 hPa geopotential height in summer (not shown) show a cyclonic circulation centered over central-eastern Asia and an anticyclonic circulation over the coast of eastern China and the adjacent oceans, leading to southeast-northwestward pressure gradients. The differences of the 850 hPa geopotential height (not shown) indicate that a weakening period of the LSTC is accompanied by an above-normal geopotential height over the East Asian continent and a below-normal one over the ocean, resulting in reduced southeast-northwestward pressure gradients, but the opposite anomaly occurs during the strengthening period of the LSTC.

Figure 11 shows the wind differences at 850 hPa during the weakening and strengthening periods of the LSTC simulated with different EACRSST forcings. A noticeable feature in Figs. 11a and 11b is that an anomalous anticyclonic pattern is found over the East Asian continent, accompanied by an anomalous northeast wind along the coast of East China, signifying the decrease of the EASM during the weakening period of the LSTC. However, an anomalous cyclonic pattern appears over the East Asian continent with an anomalous southwest wind along the coast of East

China in Figs. 11c and 11d, suggesting the increase of the EASM during the strengthening period of the LSTC. This is consistent with the pressure and air temperature gradient differences at 850 hPa.

Yoshikane and Kimura (2001) studied the formation mechanism of the Baiu front using a regional atmospheric model. They concluded that the Baiu front could be reproduced by two factors alone: the zonal mean field and the land/sea contrast. The variation of the SST in the model domain seems to be less important to the Baiu front genesis than the contrast between land and sea, but the strength of the Low-Level Jet, the amount of the precipitation and the intensity of the anti cyclonic circulation in the Pacific Ocean are strongly affected. In this study, we focus on the impacts of the EACRSST variation on the EASM. From the analyses above, it is found that the EACRSST variations affect the strength of the EASM and the amount of the precipitation strongly, which is similar to the results obtained by Yoshikane and Kimura (2001). But it is necessary to point out that different EACRSST variability forcings result in the differences of sensible and latent heat flux exchanges at the air-sea interface which alter the heating rate of the atmosphere and further lead to the air temperature differences in the lower troposphere, and the LSTC changes subsequently. The EASM increases (decreases) during
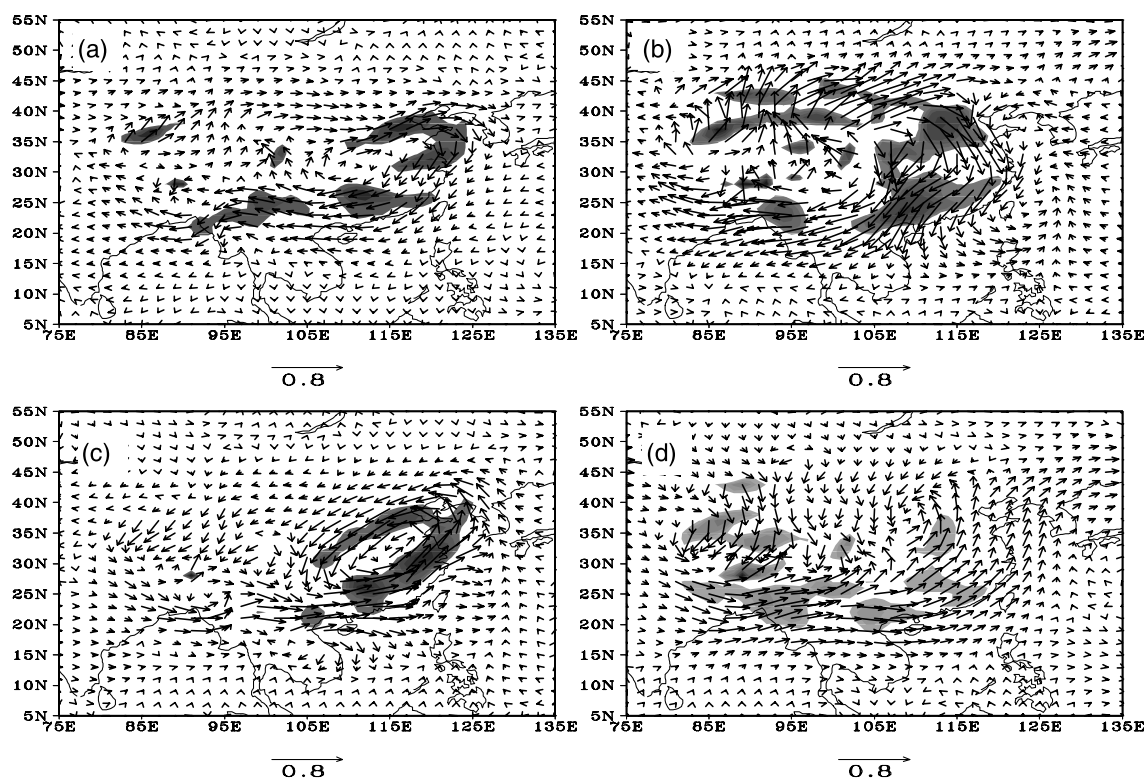
Fig. 11. As in Fig. 9, except for 850 hPa wind in summer (Units: m s^{-1}).

the strengthening (weakening) period of the LSTC.

5. Concluding remarks

The impacts of the EACRSST seasonal variability and interannual variability on the EASM are examined using a regional climate model. The results show that the PσRCM9 has a good performance in simulating the temporal evolution features of the EASM and the summer precipitation over the EASM region during the period from 1958 to 1997.

The IEASM differences between different EACRSST forcings become much larger after the mid-1970s compared to before, indicating the strengthening of the correlation between the EACRSST and the EASM after the mid-1970s. And the variability of the EACRSST forcing became much more important to the EASM interannual variability after the mid-1970s. The impacts of the EACRSST on the summer precipitation over each sub-region in the EASM region become weak gradually from south to north, and the temporal evolution features of the summer precipitation differences over North and Northeast China agree well with those of the IEASM differences after 1980: the summer precipitation over North and Northeast China decreases during the weakening period of the EASM, but the opposite anomaly occurs during the

strengthening period of the EASM.

Different EACRSST forcings result in the differences of sensible and latent heat flux exchanges between air and sea, which alter the heating rate of the atmosphere. The heating rate differences induce low level air temperature differences over East Asia, and the LSTC changes subsequently, which leads to the 850 hPa geopotential height differences. When the 850 hPa geopotential height increases over the East Asian continent and decreases over the coast of East China and the adjacent oceans during the weakening period of the LSTC, the southeast-northwestward pressure gradients decrease and the EASM weakens consequently. On the contrary, the EASM intensifies during the strengthening period of the LSTC.

REFERENCES

Anthes, R. A., 1977: A cumulus parameterization scheme utilizing a one-dimensional cloud model. *Mon. Wea.*

Rev., **105**(3), 270–286.

Ding Yihui, 1994: Summer monsoon rainfall in China and its regional characteristics, *Asian Monsoon*, China Meteorological Press, Beijing, China, 76–83. (in Chinese)

Guo Qiyun, 1994: Monsoon and the droughts and floods in China. *Asian Monsoon*, China Meteorological Press, Beijing, China, 65–74. (in Chinese)

Guo Qiyun, Cai Jingning, Shao Xuemei, and Sha Wanying, 2003: Interdecadal variability of East-Asian summer monsoon and its impact on the climate of China. *Acta Geographica Sinica*, **58**(4), 569–576. (in Chinese)

Huang Anning, and Zhang Yaocun, 2004: Impacts of seasonal and interannual variability of sea surface temperature on the climate variability over East Asia. *Journal of Nanjing University* (Natural Sciences), **40**(3), 319–329. (in Chinese)

Huang, R., and F. Sun, 1992: Impact of the tropical western Pacific on the East Asian summer monsoon. *J. Meteor. Soc. Japan*, **70**(1B), 243–256.

Huang Ronghui, and Sun Fengying, 1994: Impacts of the thermal state and the convective activities in the tropical western warm pool on the summer climate anomalies in East Asia. *Scientia Atmospherica Sinica*, **18**(2), 141–151. (in Chinese)

Huang Ronghui, and Huang Gang, 1999: Advances and problems needed for further investigation in the studies of the East Asian summer monsoon. *Chinese J. Atmos. Sci.*, **23**(2), 129–141. (in Chinese)

Huang Ronghui, Zhou Liantong, and Chen Wen, 2003: The progresses of recent studies on the variabilities of the East Asian monsoon and their causes. *Adv. Atmos. Sci.*, **20**(1), 55–69.

Huang Ronghui, Gu Lei, Xu Yuhong, Zhang Qilong, Wu Shangsen, and Cao Jie, 2005: Characteristics of the interannual variations of the onset and advance of the East Asian summer monsoon and their associations with thermal states of the tropical western Pacific. *Chinese J. Atmos. Sci.*, **29**(1), 20–36. (in Chinese)

Jin Zuhui, and Chen Jun, 2002: A composite study of the influence of SST warm anomalies over the western Pacific warm pool on Asian summer monsoon. *Chinese J. Atmos. Sci.*, **26**(1), 57–68. (in Chinese)

Kalnay, E., and Coauthors, 1996: The NCEP/NCAR 40-year reanalysis project. *Bull. Amer. Meteor. Soc.*, **77**, 437–471.

Kuo H. L., and Y. F. Qian, 1981: Influence of the Tibetan Plateau on cumulative and diurnal changes of weather and climate in summer. *Mon. Wea. Rev.*, **109**, 2337–2356.

Kuo H. L., and Y. F. Qian, 1982: Numerical simulation of the development of mean monsoon circulation in July. *Mon. Wea. Rev.*, **110**, 1879–1897.

Kurihara, K., 1989: A climatological study on the relationship between the Japanese summer weather and the subtropical high in the western northern Pacific. *Geophys. Mag.*, **43**, 45–104.

Li Feng, and He Jinhai, 2001: SST interdecadal change over Pacific area and its relation to East Asian summer monsoon. *Scientia Meteorologica Sinica*, **21**(1), 28–35. (in Chinese)

Li Feng, and He Lifu, 2002: Study of inter-decadal/interannual variation of rainfall over mid-lower reaches of Changjiang River and its mechanism. *Journal of Applied Meteorological Science*, **13**(5), 718–726. (in Chinese)

Liang Jianyin, and Wu Shansen, 2003: The study on the mechanism of SSTA in the Pacific Ocean affecting the onset of summer monsoon in the South China Sea. *Acta Oceanologica Sinica*, **25**(1), 28–41. (in Chinese)

Liu Huaqiang, and Qian Yongfu, 1999: Numerical simulation of intense Meiyu rainfall in 1991 over the Changjiang and Huaihe River valleys by a regional climate model with P-σ incorporated coordinate system. *Adv. Atmos. Sci.*, **16**(3), 395–404.

Liu Huaqiang, Qian Yongfu, and Zheng Yiqun, 2002: Effects of nested area size upon regional climate model simulations. *Adv. Atmos. Sci.*, **19**(1), 111–120.

Lu Junmei, Ren Juzhang, and Ju Jianhua, 2004: The interdecadal variability of East Asian summer monsoon and its effect on the rainfall over China. *Journal of Tropical Meteorology*, **20**(1), 73–80. (in Chinese)

Nitta, T., 1987: Convective activities in the tropical western Pacific and their impact on the Northern Hemisphere summer circulation. *J. Meteor. Soc. Japan*, **64**, 373–390.

Qian Yongfu, 1985: A fiver-layer primitive equation model with topography. *Plateau Meteorology*, **4**(2), 1–28. (in Chinese)

Qian Yongfu, Zheng Yiqun, and M. Q. Miao, 2003: Responses of China's summer monsoon climate to snow anomaly over the Tibetan Plateau. *Int. J. Climatol.*, **23**, 593–613.

Ren Xuejuan, and Qian Yongfu, 1999: Basic climatological features of air-sea heat exchanges in the South China Sea region and their relations with the SCS monsoon. *Acta Meteor. Sinica*, **13**(4), 426–438.

Ren Xuejuan, and Qian Yongfu, 2005: A coupled regional air-sea model, its performance and climate drift in simulation of the East Asian summer monsoon in 1998. *Int. J. Climatol.*, **25**, 679–692.

Shi Neng, Zhu Qiangen, and Wu Bingui, 1996: The East Asian summer monsoon in relation to summer large scale weather climate anomaly in China for last 40 years. *Scientia Atmospherica Sinica*, **20**(5), 575–583. (in Chinese)

Sun Shuqing, and Ma Shujie, 2003: Analysis and numerical experiment on the relationship between the 1998 summer monsoon activities and SSTA in tropical regions. *Chinese J. Atmos. Sci.*, **27**(1), 36–52. (in Chinese)

Sun Xiurong, Chen Longxun, and He Jinhai, 2002: Index of the land-sea thermal difference and its relation to the interannual variation of summer circulation and rainfall over East Asia. *Acta Meteor. Sinica*, **60**(2), 164–172. (in Chinese)

Sun Ying, and Ding Yihui, 2003: A study on physical

mechanisms of anomalous activities of East Asian summer monsoon during 1999. *Acta Meteorologica Sinica*, **61**(4), 406–420. (in Chinese)

Wang Huijun, 2000: The interannual variability of the East Asian monsoon and its relation with SST in a coupled atmosphere-ocean-land climate model. *Adv. Atmos. Sci.*, **17**, 31–47.

Wang Huijun, 2001a: The weakening of the Asian monsoon circulation after the end of 1970's. *Adv. Atmos. Sci.*, **18**(3), 376–386.

Wang Qianqian, and Qian Yongfu, 1995: Numerical experiments of the effects of sea surface temperature anomalies over the Pacific in 1991. *Acta Meteor. Sinica*, **9**(2), 207–214.

Wang Shiyu, 2001b: Diagnostic analyses of summer monsoon and numerical studies of regional climate change in East Asia. Ph. D. dissertation, Department of Atmospheric Sciences, Nanjing University, 23–32. (in Chinese)

Wang Shiyu, and Qian Yongfu, 2002: The effects of vertical resolution of P-σ coordinate regional climate model on simulated results. *Plateau Meteorology.* **20**(1), 28–35. (in Chinese)

Xue Feng, 2001: Interannual to interdecadal variation of East Asian summer monsoon and its association with global atmospheric circulation and sea surface temperature. *Adv. Atmos. Sci.*, **18**(4), 567–575.

Yoshikane T., and F. Kimura, 2001: Numerical study on the Baiu front genesis by heating contrast between land and ocean. *J. Meteor. Soc. Japan*, **79**(2), 671–686.

Zhang Qiong, and Qian Yongfu, 1999: Effects of boundary layer parameterization on the monthly mean simulation. *Acta Meteorolagica Sinica*, **13**, 73–85. (in Chinese)

Zhang Weiqing, and Qian Yongfu, 2002: Simulation of the effects of the variations of sea surface temperature anomaly in the equatorial Indian Ocean on the precipitation in China. *Chinese J. Atmos. Sci.*, **26**(1), 91–101. (in Chinese)

Zhang, Y., and W. Perrie, 2001: Feedback mechanisms for the atmosphere and ocean surface. *Bound.-Layer Meteor.*, **100**, 321–348.

Zhu Jinhong, and Wang Shaowu, 2001: 80a oscillation of summer rainfall over the east part of China and East-Asian summer monsoon. *Adv. Atmos. Sci.*, **18**(5), 1043–1051.

Zhu Kezhen, 1934: Southeast monsoon and rainfall in China. *Journal of the Geographical Society of China*, **1**, 1–26. (in Chinese)

Zhu Qiangen, 1986: A study of circulation differences between East Asian and Indian summer monsoon with their interactions. *Adv. Atmos. Sci.*, **3**(4), 466–477.